Fermi arcs and pseudogap phase in a minimal microscopic model of d-wave superconductivity

Dheeraj Kumar Singh,[1] Samrat Kadge,[2] Yunkyu Bang,[3,4] and Pinaki Majumdar[2]
[1]*School of Physics and Materials Science, Thapar Institute of Engineering and Technology, Patiala-147004, Punjab, India*
[2]*Harish-Chandra Research Institute, HBNI, Chhatnag Road, Jhunsi, Allahabad 211019, India*
[3]*Department of Physics, POSTECH, Pohang, Gyeongbuk 790-784, Korea*
[4]*Asia Pacific Center for Theoretical Physics, Pohang, Gyeongbuk 790-784, Korea*

(Received 27 March 2021; revised 20 December 2021; accepted 24 January 2022; published 2 February 2022)

We conclusively show that a pseudogap state can arise at $T > T_c$, for reasonable pairing interaction strength, from order parameter fluctuations in a two-dimensional minimal model of d-wave superconductivity. The occurrence of the pseudogap requires neither strong correlation nor the presence of competing order. We study a model with attractive nearest-neighbor interaction and establish our result using a combination of a cluster-based Monte Carlo method for the order parameter field and a twisted-boundary scheme to compute the momentum-resolved spectral function. Apart from a dip in the density of states that characterizes the pseudogap, the momentum and frequency resolution on our effective lattice size $\sim 160 \times 160$ allows two major conclusions: (i) at $T < T_c$, despite the presence of thermal phase fluctuations, the superconductor has only nodal Fermi points while all non-nodal points on the normal state Fermi surface show a two-peak spectral function with a dip at $\omega = 0$, and (ii) for $T > T_c$, the Fermi points develop into arcs, characterized by a single quasiparticle peak, and the arcs connect up to recover the normal state Fermi surface at a temperature $T^* > T_c$. We show the variation of T_c and T^* with coupling strength and provide detailed spectral results at a coupling where $T^* \sim 1.5T_c$.

DOI: 10.1103/PhysRevB.105.054501

I. INTRODUCTION

Experiments on the underdoped cuprates were the first to focus attention on a "pseudogap" phase [1]. It was observed that a gap persists in the quasiparticle excitation spectrum above the superconducting transition temperature T_c. Unlike the conventional superconductors, there exists another temperature scale, $T^* > T_c$, for the disappearance of the antinodal gap [2–5]. An intriguing aspect of the spectral properties in the pseudogap (PG) phase is the appearance of Fermi arcs above T_c, while the $T < T_c$ phase shows only nodal Fermi points despite thermal phase fluctuations. The $T_c < T < T^*$ window shows partial gapping of the Fermi surface. The length of the Fermi arcs increases with temperature until the normal state Fermi surface (FS) is recovered [6–12] at T^*.

Theoretical work on this problem has explored multiple possibilities. One focuses on the fluctuation in amplitude of the d-wave superconducting (dwSC) order parameter as the origin of PG behavior [13–18]. Another—the "semiclassical approximation" (SCA)—attributes the Fermi-arc formation to a square-root singularity along the FS in the spectral function that results from the Doppler shift of the quasiparticle energy in the presence of supercurrent in the PG phase [16,19]. Later study, however, indicated that such singularity may be an artifact of the SCA, which itself may be unjustifiable because the quasiparticles are massless near the nodes in the PG region [20]. A recent work [21] considers electron self-energy correction due to the exchange of a Cooper-pair fluctuation at finite temperature. A crucial input in the theory, the correlation length $\xi(T)$, was assumed to have a phenomenological Berezinskii-Kosterlitz-Thouless (BKT) [22] form, while the temperature-dependent dwSC order parameter $\Delta(T)$ was adopted from the angle-resolved photoemission spectroscopy (ARPES) measurements.

Despite the exploration of various physical mechanisms, the microscopic origin of the PG phase in the high-T_c cuprates remains highly debated. An exact-diagonalization (ED) + Monte Carlo (MC)-based study in a microscopic model [23] pointed out that the PG phase may not exist for a realistic value of interaction, $V \sim t$ (where t is the hopping scale), in a minimal microscopic model. On the other hand, another work using a relatively larger system size suggested otherwise [24]. However, both approaches suffered from a system size that was not adequate to examine the momentum-resolved spectral function and establish the existence of Fermi arcs in the $T > T_c$ window. Another approach stressed the competing dwSC and antiferromagnetic order [25] using MC simulation of a Landau-Ginzburg (LG) functional and also considered the presence of quenched disorder [26]. The obtained order parameters were used in a microscopic model to show the existence of the PG phase. The topological aspect of this transition has also been discussed [27]. Finally, recent work indicates that the onset of the PG phase may be accompanied by the appearance of nematic order [11,28–32].

In this richly varied field, it may be useful to first conclusively establish what spectral features can emerge from purely d-wave pairing fluctuations, and only then build in additional effects. In this spirit, we explore the impact of classical thermal fluctuations of the d-wave order parameter field on the electronic spectrum. In these studies, the ED+MC method is

the most frequently used approach. However, the use of the approach is limited by the relatively small lattice size that is accessible, owing to the high computational cost [23,24]. This is a serious hindrance for examining the spectral properties, especially the momentum-resolved spectral functions along the normal state Fermi surface, an exercise essential to examine the pseudogap phase.

In this paper, we adopt an approach which uses a combination of a cluster-based MC method [33] to access thermal fluctuations on reasonably large sizes, and a twisted-boundary condition (TBC) scheme [34] to obtain high-resolution spectra. For a small system size, with poor momentum resolution, it is difficult to determine the extent of the Fermi arc. This is because only a small fraction of the momentum points fall on the FS or are close to it. Therefore, we first obtain equilibration for size $L_{MC}\times L_{MC}$ ($L_{MC}=20$) and, for spectral calculations, employ TBC—repeating an equilibrated configuration $L_{tw}=8$ times along both the x and y directions. Then, the momentum-resolved spectral function is obtained by using Bloch's theorem for a lattice of effective size $L_{\rm eff}=L_{MC}\times L_{tw}$, i.e., 160×160. We summarize our main results below in terms of the single-particle spectral function $A(\mathbf{k},\omega)$.

(i) We show the existence of a PG phase above T_c in a minimal model for dwSC without invoking the presence of any competing order, suggesting that the key difference between the PG phase and pure dwSC may be the absence of phase correlation in the former. (ii) For $T<T_c$, there is a two-peak structure in $A(\mathbf{k},\omega)$ for all momenta on the normal state Fermi surface, except the nodal points—where a quasiparticle peak is visible. The spectral weight $A(\mathbf{k},0)$ on this contour falls sharply away from the nodal points. (iii) For $T>T_c$, the single-peak quasiparticle feature is visible over a larger part of the normal state Fermi surface, forming "Fermi arcs" around the nodal points. The Fermi arcs increase in length and connect up to create the normal Fermi surface at $T=T^*$, where the two-peak feature at the antinodal point also collapses.

II. MODEL AND METHOD

A. Model

We consider a minimal two-dimensional electron model,

$$H=-\sum_{\mathbf{ij}\sigma}t_{\mathbf{ij}}d^\dagger_{\mathbf{i}\sigma}d_{\mathbf{j}\sigma}-\mu\sum_{\mathbf{i}}n_{\mathbf{i}}-|V|\sum_{\langle\mathbf{ij}\rangle}n_{\mathbf{i}}n_{\mathbf{j}}. \tag{1}$$

The first term is the kinetic energy, which includes both first- (t) and second- (t') neighbor hoppings. We set $t=1$. We choose $t'=-0.4$ so as to reproduce the experimentally observed Fermi surface [35]. In the second term, μ is the chemical potential, which is chosen to correspond to the band filling $n\sim0.9$. Finally, the last term describes the nearest-neighbor attractive interaction responsible for dwSC pairing. The interaction parameter $V\sim1.0$ is chosen so that it is consistent with the nearest-neighbor antiferromagnetic coupling $J\approx4t^2/U\sim1$. We have fixed $V=1.2$ for all the calculations, unless stated otherwise.

B. Monte Carlo strategy

The effective Hamiltonian below, employed in the simulation process, can be formally obtained via a Hubbard-Stratonovich transformation of the intersite interaction in the d-wave pairing channel and assuming the pairing field $\Delta^\delta_{\mathbf{i}}$ to be "static," i.e., classical. This is equivalent, structurally, to a "mean-field"-like decoupling of the interaction, without any additional assumption about homogeneity and phase correlation among the $\Delta^\delta_{\mathbf{i}}$. The $\Delta^\delta_{\mathbf{i}}$ are allowed both amplitude and phase fluctuations. We have ignored other possible decouplings, for example related to charge density wave, etc.:

$$\begin{aligned}H_{\rm eff}=&-\sum_{\mathbf{i},\delta',\sigma}t_{\mathbf{i},\mathbf{i}+\delta'}d^\dagger_{\mathbf{i}\sigma}d_{\mathbf{i}+\delta'\sigma}-\mu\sum_{\mathbf{i}}n_{\mathbf{i}}\\&-\sum_{\mathbf{i},\delta}[(d^\dagger_{\mathbf{i}\uparrow}d^\dagger_{\mathbf{i}+\delta\downarrow}+d^\dagger_{\mathbf{i}+\delta\uparrow}d^\dagger_{\mathbf{i}\downarrow})\Delta^\delta_{\mathbf{i}}+\text{H.c.}]+H_{cl},\\H_{cl}=&\frac{1}{V}\sum_{\mathbf{i}}|\Delta^\delta_{\mathbf{i}}|^2.\end{aligned} \tag{2}$$

Here, δ' refers to both the first- and second-nearest neighbors, whereas δ to only the first neighbor. The superconducting gap function defined on the link is a complex classical field and can be expressed as $\Delta^\delta_{\mathbf{i}}=|\Delta_{\mathbf{i}}|e^{i\phi^\delta}$. For simplification, $|\Delta_{\mathbf{i}}|$ is treated as a site variable, while ϕ^δ ($\delta=x,y$) is treated as a link variable.

The equilibrium configurations $\{\Delta_i,\phi^x_i,\phi^y_i\}$ are determined using the Metropolis algorithm, which involves updating the configuration according to the distribution

$$P\{\Delta_i,\phi^x_i,\phi^y_i\}\propto\text{Tr}_{dd^\dagger}e^{-\beta H_{\rm eff}}. \tag{3}$$

For an update at a given site, the Hamiltonian corresponding to a cluster of size $L_C\times L_C$ around the update site is diagonalized (using periodic boundary condition), instead of the full 20×20 system Hamiltonian. We use $L_C=6$. This approximation is based on the assumption that the effect of the proposed change at the update site decreases quickly with distance as one moves away [36]. Benchmarked earlier for spin-fermion and other similar models, it leads to a significant reduction in update cost from $\sim N^3$ to $\sim N_c^3$ for a system and cluster with N and N_c sites, respectively [33]. After equilibration, we consider a superlattice constructed using dwSC field configurations on the $L_{MC}\times L_{MC}$ system and study the spectral properties by using Bloch's theorem, as discussed in later sections.

For the interaction parameter considered in this work, we start MC simulations at a temperature $T\sim0.05t$ that is far above the dwSC transition temperature and reduce the temperature to cool down the system in steps of $\Delta T=0.0013t$. The small temperature step ensures that the system avoids any metastable states during the annealing process.

C. T_c determination

From the equilibrium configurations at a given temperature, we can calculate the long-range phase correlation $\Phi(L_{MC}/2,0)$:

$$\Phi(s_x,s_y)=\frac{1}{N}\sum_{\mathbf{i}}\langle e^{i\phi^x_{\mathbf{i}}}e^{i\phi^x_{\mathbf{i}+\mathbf{s}}}\rangle. \tag{4}$$

The T_c for dwSC is determined from the the rise of $\Phi(L_{MC}/2, 0)$ on reducing T from a high temperature. To keep track of any deviation from the dwSC state, we calculated another useful correlation function $\Psi = \frac{1}{N}\sum_{\mathbf{i}}\langle e^{i\phi_{\mathbf{i}}^x} e^{i\phi_{\mathbf{i}}^y}\rangle$. A negative Ψ indicates whether or not the state obtained in the equilibration is a dwSC state. For the interaction parameters considered in the current work, only the dwSC state is obtained.

An earlier proposal for the determination of the onset temperature T^* of the PG phase focused on the short-range phase correlation function such as $\Phi(1, 0)$, with $\Phi(1, 0) \sim 0.1$ set as a criterion for T_c. The inference [23] was that for a realistic $V \sim 1$, no PG is possible. However, the validity of such assumptions was not checked by examining the spectral function, which was challenging due to the finite-size effect.

D. Spectral features

Once the thermal equilibrium is achieved, we use the twisted-boundary condition to calculate the density of states. For instance, $t_{\mathbf{ij}} \to t_{\mathbf{ij}} e^{-i(q_x a_x + q_y a_y)}$, where $q_x, q_y = 0, 2\pi/N_l, 4\pi/N_l, \ldots, 2\pi(N_l - 1)/N_l$. $N_l = L_{tw} = 8$ is the number of lattices in the superlattice, i.e., number of repetitions along the x and y directions of the lattice under consideration in both directions. Note that we set $a_x = a_y = 1$. Similarly, $\Delta_{\mathbf{i}}^{\delta} = |\Delta_{\mathbf{i}}| e^{i\phi^{\delta}} = |\Delta_{\mathbf{i}}| e^{i\phi^{\mathbf{ij}}} = |\Delta_{\mathbf{i}}| e^{i\phi^{\mathbf{ij}}} e^{-i(q_x a_x + q_y a_y)}$ at the boundaries. Then, the density of states (DOS) is calculated as

$$N(\omega) = \sum_{\mathbf{q},\lambda,\mathbf{i}} [|u_{\mathbf{q},\lambda}(\mathbf{i})|^2 \delta(\omega - E_{\mathbf{q},\lambda}) + |v_{\mathbf{q},\lambda}(\mathbf{i})|^2 \delta(\omega + E_{\mathbf{q},\lambda})], \quad (5)$$

where $E_{\mathbf{q},\lambda}$ are the eigenvalues of the Hamiltonian obtained from Eq. (1) using the Bogoliubov-Valatin transformation. $|u_{\mathbf{q},\lambda}\rangle$ and $|v_{\mathbf{q},\lambda}\rangle$ form the eigenvectors of the Hamiltonian. The single-particle spectral function is calculated as

$$A(\mathbf{k}, \omega) = \sum_{\mathbf{q},\lambda} [|\langle \mathbf{k}|u_{\mathbf{q},\lambda}\rangle|^2 \delta(\omega - E_{\mathbf{q},\lambda}) + |\langle \mathbf{k}|v_{\mathbf{q},\lambda}\rangle|^2 \delta(\omega + E_{\mathbf{q},\lambda})], \quad (6)$$

where

$$\langle \mathbf{k}|u_{\mathbf{q},\alpha}\rangle = \sum_l \sum_i \langle \mathbf{k}|l, i\rangle \langle l, i|u_{\mathbf{q},\lambda}\rangle. \quad (7)$$

Here, l is the superlattice index and i is a site index within the superlattice.

III. RESULTS

Figure 1(a) shows both long- and short-range phase correlations, $\Phi(L_{MC}/2, 0)$ and $\Phi(1, 0)$, as a function of temperature. On decreasing temperature, $\Phi(L_{MC}/2, 0)$ starts to rise from a nearly zero value at $T_c \sim 0.035t$. $\Phi(1, 0)$ is ∼0.1 for a large temperature window above T_c for the model in this work.

One of the earliest experimental signatures of the pseudogap was a dip in the density of state (DOS) persistent above T_c, obtained in the scanning tunneling spectroscopy (STS) measurement [4]. We find a qualitatively similar dip as shown in Fig. 1(b), which retains its V-shape structure even above T_c. The dip becomes shallow enough to become unnoticeable only at temperature $T \sim 1.5T_c$, for $V = 1.2$. We estimate T^* as the temperature at which the dip in the DOS becomes unnoticeable.

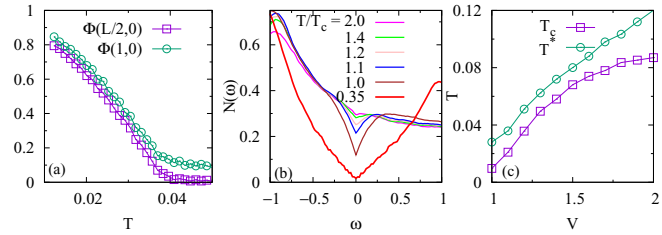

FIG. 1. (a) Long-range and short-range phase correlation function as a function of temperature. (b) Evolution of DOS as a function of temperature. The dip in the V-shaped DOS continues to exist beyond T_c and can be noticed up to $T \sim 1.5T_c$. (c) T and T^* as a function of interaction V, where the critical interaction strength $V_c \sim 1.0$ for the onset of d-wave superconductivity.

Based on that criterion, our estimate of T^* reveals its dependence on V to be similar to that of $T_c(V)$ in the intermediate-coupling regime, with the $T^*(V)$ curve running almost parallel to the T_c curve [Fig. 1(c)]. Importantly, T^*/T_c grows with a decrease in the interaction parameter V, i.e., the relative temperature window for the pseudogap phase is larger [37] for realistic $V \sim 1$.

Figure 2 shows the dependence of the long-range phase correlation function and density of states on the lattice size. The phase correlation shows only a relatively small suppression with increasing lattice size in the vicinity of the onset temperature of dwSC [Fig. 2(a)]. For temperature $T = 0.5T_c$, Fig. 2(b) shows the lattice size dependence of the density of states at temperature $T = 0.5T_c$. We compare sizes 16×16, 20×20, and the results for an effective lattice size 160×160 (using twisted-boundary conditions). The effective lattice is equivalent to an equilibrated field configurations on a 20×20 lattice size repeated eight times along both the x and y directions. The finite-size artifacts are absent in the latter, while they are significant in the two smaller sizes.

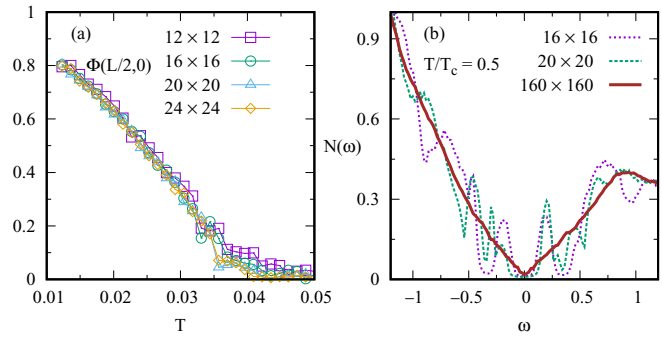

FIG. 2. (a) Phase correlation functions as a function of temperature for different lattice sizes $L_{MC} \times L_{MC}$, with $L_{MC} = 12$, 16, 20, and 24. (b) DOS for $L_{MC} = 16$ and 20 with $L_{tw} = 1$. For comparison, the DOS is also shown for $L_{MC} = 20$ and $L_{tw} = 8$, i.e., an effective lattice size of 160×160.

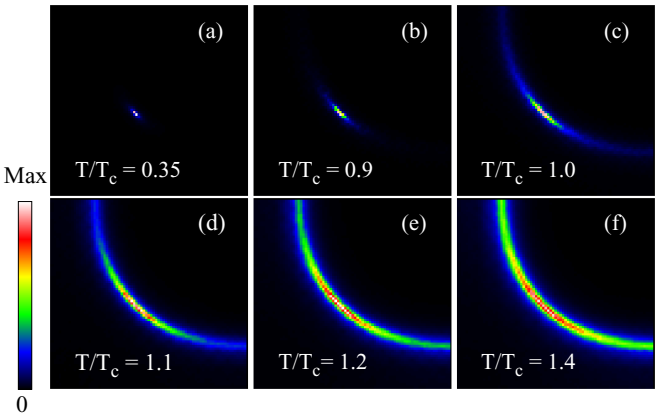

FIG. 3. Evolution of quasiparticle spectral weight $\mathcal{A}(\mathbf{k}, \omega)$ for $\omega = 0$ as a function of temperature. k_x and k_y are along horizontal and vertical directions, respectively, with each having range $[0, \pi]$. $\mathcal{A}(\mathbf{k}, 0)$ increases continuously with temperature away from the nodes. However, it is only a tiny fraction ($\sim$1%) of that in the vicinity of the node, a feature noticeable even beyond T_c, which is an indication of a preformed Cooper-pair state existing up to a very high temperature.

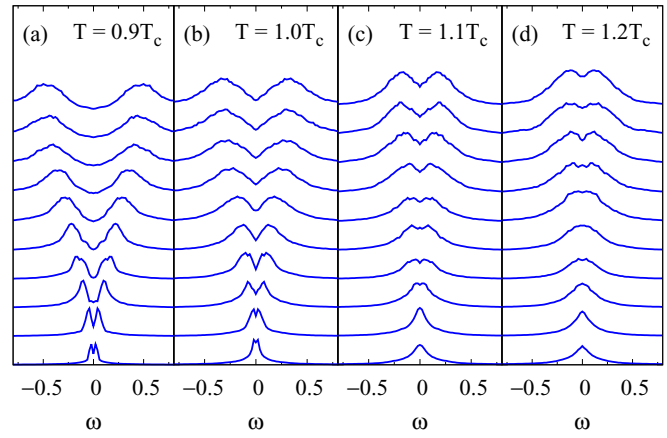

FIG. 4. Momentum-resolved spectral function $\mathcal{A}(\mathbf{k}, \omega)$ at different temperatures calculated for several values of momentum $\mathbf{k}$ along the Fermi surface ($V = 1.2$). The bottom curve in each case corresponds to a point very close to the nodal point, while the top curves correspond to a point in the vicinity of the antinode. Nodal quasiparticles are protected against the phase fluctuation below T_c and the Fermi arcs are formed above T_c that continue to exist for $T \gtrsim 1.4T_c$. Asymmetry present in the spectral function, more visible when the gap is small, is an artifact of the finite size of the system. The peak height is arbitrarily scaled to enhance the visibility.

Figure 3 shows that well below T_c, the spectral weight is concentrated at the nodal point. On approaching T_c, the spectral weight continuously builds up at points near the nodal points along the normal state FS. We will examine the energy dependence of the spectral functions further on. The weight at points on the nominal FS away from the nodal point remains only a tiny fraction ($\sim$1%) of that at the node. The process of spectral weight buildup continues beyond T_c. The spectral weight remains highest near the nodal points and smallest near the antinodal, even beyond T^*, which clearly indicates the existence of Cooper pairs without any phase coherence between them. Above T_c, the pseudogap can be expected to quickly fill, first near the nodal points and then away from them, until the whole of the normal state Fermi surface appears.

To understand how the gaps are filled away from the nodal points either below or above T_c, we examine the momentum-resolved spectral function as plotted in Fig. 4 for the points ($\mathbf{k}$) along the normal state FS. Because of the finite-size effect, most of the points are slightly away from the normal state FS (within the range of $\Delta k_x = \Delta k_y \lesssim 0.03$). It introduces small asymmetry, which is removed by plotting the symmetrized spectral functions $[\mathcal{A}(\mathbf{k}, \omega) + \mathcal{A}(\mathbf{k}, -\omega)]/2$ instead.

Several points are to be noted. First of all, the SC order parameter retains its d-wave character below T_c, despite phase fluctuations. A two-peak structure exists with a small dip at $\omega = 0$ for any non-nodal point, however close they are to the nodes, all the way up to T_c. It indicates that the Fermi points remain intact against the thermal phase fluctuations below T_c. This is in contrast to the mean-field picture in which the dwSC order parameter approaches zero all along the normal state FS while preserving its d-wave symmetry. Second, the spectral weight continuously increases as the temperature increases at the points near the nodes, along the normal state FS. This is also accompanied by the disappearance of the dip associated with the thermally broadened two-peak structure and appearance of a single broad peak, starting from the points in the vicinity of the nodal points and extending up to those near the antinodal points, as T increases beyond T_c and reaches T^*. Thus, the region $T_c < T < T^*$ is marked by the spectral features which are in qualitative agreement with the ARPES measurements [8].

We have found that the peak in the dwSC amplitude distribution shows only a small shift across the entire temperature range considered here. We find $\Delta_{an}(T_c) \approx 0.5\Delta_{an}(0)$, while $\Delta_{an}(T)$ does not noticeably decrease within the range $T_c \lesssim T \lesssim T^*$. The feature, which is indicative of the PG as a preformed Cooper-pair state without the absence of any phase coherence, also agrees with the ARPES measurements according to which $\Delta_{an}(T)$ remains independent of temperature for the entire range $0 < T < T^*$. For us, however, $\Delta_{an}(T)$ shows a drop in size by nearly one-half on approaching T_c from below.

Figure 5 shows the thermally averaged spectral function $\mathcal{A}(\mathbf{k}, -\omega) + \mathcal{A}(\mathbf{k}, \omega)$. The existence of banana-shaped constant energy surfaces can be seen nearly up to T_c. These banana-shaped constant energy surfaces within the octet model have been used to explain the features of quasiparticle interference in the superconducting cuprates [38].

In this paper, we focused on a particular electron density corresponding to "hole doping" $x \approx 0.1$ on the half-filled state. However, we ignored correlation effects that lead to the Mott state at half-filling and also the possibility of competing phases such as magnetic and charge order. These effects are essential for any detailed understanding of the underdoped cuprates. We touch upon this next in our discussion.

IV. CONNECTION TO EXPERIMENTS

Having discussed our results, we would like to place them in the context of the pseudogap effect observed in the cuprates.

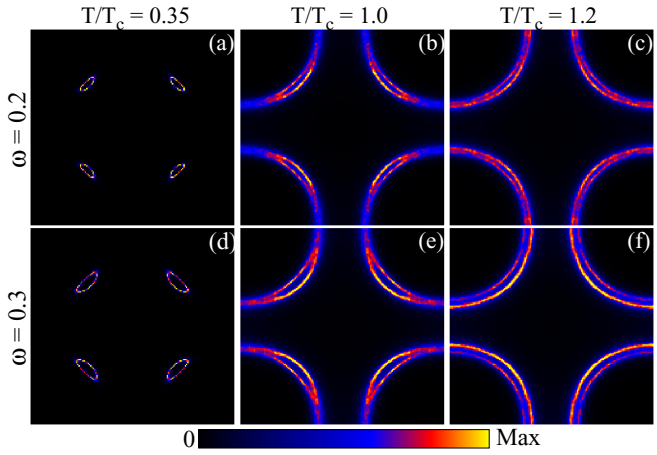

FIG. 5. Thermally averaged $\mathcal{A}(\mathbf{k}, -\omega) + \mathcal{A}(\mathbf{k}, \omega)$ for k_x and k_y in the range $[-\pi, \pi]$. The columns are for temperatures $T/T_c = 0.35$, 1, and 1.2, while the rows show data at $\omega = 0.2$ and 0.3, respectively.

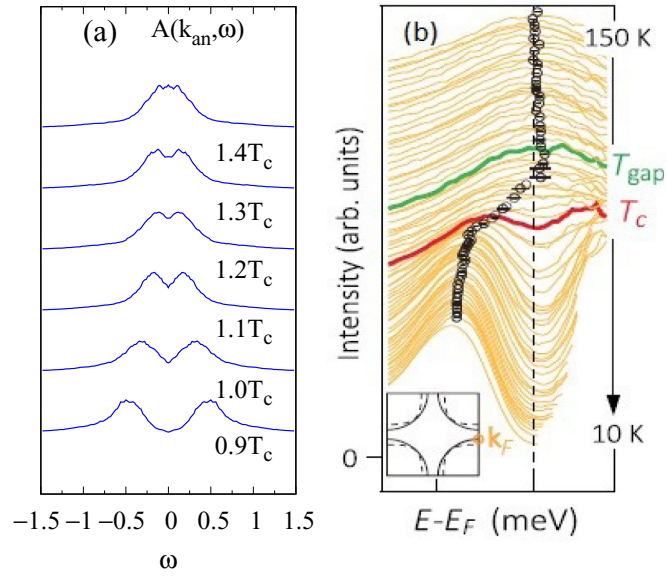

FIG. 6. (a) Calculated and (b) experimentally determined antinodal quasiparticle energy distribution curve $\mathcal{A}(\mathbf{k}_{an}, \omega)$ as a function of temperature [41]. Experimental data are for an overdoped sample.

There are two distinct regimes of "pseudogap physics" as brought out by recent photoemission experiments. The first pertains to the well-studied underdoped regime, where the proximity to the $x = 0$ Mott insulator and competing charge and spin order plays a role. The other, more pertinent to us, occurs at relatively high doping, $x \gtrsim 0.19$, where the "competing order" effects are weak and one may be looking purely at d-wave pairing fluctuations. Below, we first comment on the underdoped regime, where we really cannot make any quantitative comment, and then at the large doping window.

A. The underdoped regime

The underdoped cuprates exhibit a wide variety of symmetry-breaking phenomena, including charge order, nematic order, and breaking of time-reversal as well as inversion symmetry, well above the superconducting transition temperature [39]. The occurrence of these correlations also coincides with the presence of a dip in the DOS. There is no quasiparticle peak at the antinodal point above T_c and a pseudogap appears on approaching T_c marked by the existence of *Fermi arcs*. The length of the Fermi arc continues to decrease, and vanishes at T_c, when it gets transformed to Fermi points. Our results show a qualitative agreement with this experimental feature, though the size of the gap rapidly decreases with temperature beyond T_c [8].

Correlation effects in the underdoped window can be approximately incorporated within the Gutzwiller scheme that renormalize the hopping amplitude t and pairing interaction V. The respective factors are $g_t = 2x/(1+x)$ and $g_s = 4/(1+x)^2$, where x is the hole doping. The effective hopping vanishes as $x \to 0$, while the pairing interaction saturates. The ratio $\tilde{V}/\tilde{t} = (V/t) * 2/[x(1+x)]$. This suggests that the effective V/t is significantly enhanced for $x = 0.1$ used in this work.

One can look at the consequence of this in two ways, with a similar qualitative conclusion. (i) Correlation effects would suppress charge fluctuations, and the kinetic energy, in the doped Mott insulator. As suggested by pairing stiffness calculations in the projected ground state [40], the T_c would be strongly suppressed with respect to its "uncorrelated" value, with $T_c \to 0$ as $x \to 0$. This opens up a large window between T_c and the "pairing scale" decided by V. The pseudogap window increases because the T_c gets lowered. Alternately, (ii) one can look at an uncorrelated system with V/t now renormalized by g_s/g_t. It has been pointed out [23] that the temperature window for the pseudogap phase increases with increasing V/t. Our Fig. 1(b) shows the effect. Overall, the pseudogap window will widen at small x, compared to the estimate we make, due to the T_c suppression caused by correlation effects.

B. The large doping regime

Beyond the underdoping window, the state above the superconducting dome is expected to be a normal metal marked by the presence of a well-defined quasiparticle peak all along the Fermi surface. On the contrary, recent work [39,41] indicates the persistence of an antinodal gap in the spectral function above T_c, a feature suggested to be intrinsic to a dwSC [Fig. 6(b)]. However, there is a marked difference from the usual pseudogap phase: the lowering of temperature is accompanied first with a sharpening of the quasiparticle peak before the gap appears close to, but above, the superconducting transition. Our calculations, which only take d-wave correlations and no competing order into account, show a behavior akin to what is observed in the ARPES spectrum for the antinodal point in the overdoped region [Fig. 6(a)]. First, we find that the antinodal spectrum is gapped above T_c. Second, the gap closes rapidly with an increase in temperature and disappears beyond $\sim 1.5T_c$ with the appearance of antinodal quasiparticles.

V. CONCLUSIONS

We have explored the possibility of a pseudogap phase in a minimal microscopic model of d-wave superconductivity.

We established the dependence of T_c and the pseudogap onset temperature T^* on the pairing interaction V and found that for V typical of the cuprates, the antinodal two-peak structure, with a shallow dip in between, persists in the momentum-resolved spectrum up to $T^* \sim 1.5T_c$. We observe that despite thermal fluctuations, an essentially nodal Fermi surface is seen for $T < T_c$, while for $T > T_c$, there is a Fermi arc feature, characterized by thermally broadened quasiparticle peaks, around the nodal points. The arcs increase in length from T_c to T^*, where they connect up to recover the normal state Fermi surface. Around T^*, the two-peak feature in the antinodal spectral function also collapses into a single-peak feature. We provide a comprehensive map of the spectral function for varying momentum and temperature. The technical innovations used in this work can serve as the starting point for more elaborate models where the role of competing channels, of density order or magnetism, can be studied in conjunction with d-wave superconductivity.

ACKNOWLEDGMENTS

D.K.S. was supported through DST/NSM/R&D_HPC_Applications/2021/14 funded by DST-NSM; start-up research grant SRG/2020/002144 funded by DST-SERB; seed-project grant TU/DORSP/57/2299 funded by TIET and he would like to thank A. Akbari for useful discussions. Y.B. was supported through NRF Grant No. 2020-R1A2C2-007930 funded by the National Research Foundation of Korea. We acknowledge use of the HPC facility at HRI.

[1] N. J. Robinson, P. D. Johnson, T. M. Rice, and A. M. Tsvelik, Rep. Prog. Phys. **82**, 126501 (2019).
[2] H. Ding, T. Yokoya, J. C. Campuzano, T. Takahashi, M. Ran- deria, M. R. Norman, T. Mochiku, K. Kadowaki, and J. Giapintzakis, Nature (London) **382**, 51 (1996).
[3] A. G. Loeser, Z.-X. Shen, D. S. Dessau, D. S. Marshall, C. H. Park, P. Fournier, and A. Kapitulnik, Science **273**, 325 (1996).
[4] C. Renner, B. Revaz, J.-Y. Genoud, K. Kadowaki, and O. Fischer, Phys. Rev. Lett. **80**, 149 (1998).
[5] M. R. Norman, H. Ding, M. Randeria, J. C. Campuzano, T. Yokoya, T. Takeuchi, T. Takahashi, T. Mochiku, K. Kadowaki, and P. Guptasarma, Nature (London) **392**, 157 (1998).
[6] T. Yoshida, X. J. Zhou, T. Sasagawa, W. L. Yang, P. V. Bogdanov, A. Lanzara, Z. Hussain, T. Mizokawa, A. Fujimori, H. Eisaki, Z.-X. Shen, T. Kakeshita, and S. Uchida, Phys. Rev. Lett. **91**, 027001 (2003).
[7] A. Kanigel, M. R. Norman, M. Randeria, U. Chatterjee, S. Souma, A. Kaminski, H. M. Fretwell, S. Rosenkranz, M. Shi, T. Sato, T. Takahashi, Z. Z. Li, H. Raffy, K. Kadowaki, D. Hinks, L. Ozyuzer, and J. C. Campuzano, Nat. Phys. **2**, 447 (2006).
[8] A. Kanigel, U. Chatterjee, M. Randeria, M. R. Norman, S. Souma, M. Shi, Z. Z. Li, H. Raffy, and J. C. Campuzano, Phys. Rev. Lett. **99**, 157001 (2007).
[9] M. Hashimoto, I. M. Vishik, R.-H. He, T. P. Devereaux, and Z.-X. Shen, Nat. Phys. **10**, 483 (2014).
[10] T. Kondo, W. Malaeb, Y. Ishida, T. Sasagawa, H. Sakamoto, T. Takeuchi, T. Tohyama, and S. Shin, Nat. Commun. **6**, 7699 (2015).
[11] Y. Sato, S. Kasahara, H. Murayama, Y. Kasahara, E.-G. Moon, T. Nishizaki, T. Loew, J. Porras, B. Keimer, T. Shibauchi, and Y. Matsuda, Nat. Phys. **13**, 1074 (2017).
[12] N. Doiron-Leyraud, O. Cyr-Choiniére, S. Badoux, A. Ataei, C. Collignon, A. Gourgout, S. Dufour-Beausejour, F. F. Tafti, F. Laliberté, M.-E. Boulanger, M. Matusiak, D. Graf, M. Kim, J.-S. Zhou, N. Momono, T. Kurosawa, H. Takagi, and L. Taillefer, Nat. Commun. **8**, 2044 (2017).
[13] M. Randeria, N. Trivedi, A. Moreo, and R. T. Scalettar, Phys. Rev. Lett. **69**, 2001 (1992).
[14] V. J. Emery and S. A. Kivelson, Nature (London) **374**, 434 (1995).
[15] M. R. Norman, M. Randeria, H. Ding, and J. C. Campuzano, Phys. Rev. B **57**, R11093 (1998).
[16] M. Franz and A. J. Millis, Phys. Rev. B **58**, 14572 (1998).
[17] H.-J. Kwon and A. T. Dorsey, Phys. Rev. B **59**, 6438 (1999).
[18] W. A. Atkinson, J. D. Bazak, and B. M. Andersen, Phys. Rev. Lett. **109**, 267004 (2012).
[19] E. Berg and E. Altman, Phys. Rev. Lett. **99**, 247001 (2007).
[20] M. Khodas and A. M. Tsvelik, Phys. Rev. B **81**, 094514 (2010).
[21] S. Banerjee, T. V. Ramakrishnan, and C. Dasgupta, Phys. Rev. B **84**, 144525 (2011).
[22] P. Olsson, Phys. Rev. B **52**, 4526 (1995).
[23] M. Mayr, G. Alvarez, C. Sén, and E. Dagotto, Phys. Rev. Lett. **94**, 217001 (2005).
[24] Y.-W. Zhong, T. Li, and Q. Han, Phys. Rev. B **84**, 024522 (2011).
[25] A. Paramekanti and E. Zhao, Phys. Rev. B **75**, 140507(R) (2007).
[26] G. Alvarez and E. Dagotto, Phys. Rev. Lett. **101**, 177001 (2008).
[27] C. M. Varma and L. Zhu, Phys. Rev. Lett. **98**, 177004 (2007).
[28] H. Murayama, Y. Sato, R. Kurihara, S. Kasahara, Y. Mizukami, Y. Kasahara, H. Uchiyama, A. Yamamoto, E.-G. Moon, J. Cai, J. Freyermuth, M. Greven, T. Shibauchi, and Y. Matsuda, Nat. Commun. **10**, 3282 (2019).
[29] S. Mukhopadhyay, R. Sharma, C. K. Kim, S. D. Edkins, M. H. Hamidian, H. Eisaki, S. Uchida, E.-A. Kim, M. J. Lawler, A. P. Mackenzie, J. C. S. Davis, and K. Fujita, Proc. Natl. Acad. Sci. USA **116**, 13249 (2019).
[30] S. A. Kivelson and S. Lederer, Proc. Natl. Acad. Sci. USA **116**, 14395 (2019).
[31] P. Choubey, S. H. Joo, K. Fujita, Z. Du, S. D. Edkins, M. H. Hamidian, H. Eisaki, S. Uchida, A. P. Mackenzie, J. Lee, J. C. S. Davis, and P. J. Hirschfeld, Proc. Natl. Acad. Sci. USA **117**, 14805 (2020).
[32] W.-L. Tu and T.-K. Lee, Sci. Rep. **9**, 1719 (2019).
[33] S. Kumar and P. Majumdar, Eur. Phys. J. B **50**, 571 (2006).
[34] J. Salafranca, G. Alvarez, and E. Dagotto, Phys. Rev. B **80**, 155133 (2009).
[35] A. Damascelli, Z. Hussain, and Z.-X. Shen, Rev. Mod. Phys. **75**, 473 (2003).
[36] W. Kohn, Phys. Rev. Lett. **76**, 3168 (1996).
[37] R. Micnas, J. Ranninger, S. Robaszkiewicz, and S. Tabor, Phys. Rev. B **37**, 9410 (1988).

[38] T. Hanaguri, Y. Kohsaka, M. Ono, M. Maltseva, P. Coleman, I. Yamada, M. Azuma, M. Takano, K. Ohishi, and H. Takagi, Science **323**, 923 (2009).

[39] S.-D. Chen, M. Hashimoto, Y. He, D. Song, K.-J. Xu, J.-F. He, T. P. Devereaux, H. Eisaki, D.-H. Lu, J. Zaanen, and Z.-X. Shen, Science **366**, 1099 (2019).

[40] A. Paramekanti, M. Randeria, and N. Trivedi, Phys. Rev. Lett. **87**, 217002 (2001).

[41] Y. He, S.-D. Chen, Z.-X. Li, D. Zhao, D. Song, Y. Yoshida, H. Eisaki, T. Wu, X.-H. Chen, D.-H. Lu, C. Meingast, T. P. Devereaux, R. J. Birgeneau, M. Hashimoto, D.-H. Lee, and Z.-X. Shen, Phys. Rev. X **11**, 031068 (2021).